Individual differences in white matter microstructure reflect variation in functional connectivity during action choice

Boorman, ED[1,2], O'Shea J [1,2], Sebastian C[2], Rushworth MFS[1,2], Johansen-Berg H[1]

[1]Centre for Functional MRI of the Brain, University of Oxford, Oxford, UK

[2]Dept of Experimental Psychology, University of Oxford, Oxford, UK

Corresponding author:
Erie Boorman
Department of Experimental Psychology
Oxford
OX1 3UD
UK

Tel: +44 (0)1865 222309
Fax: +44 (0)1865 310447

Email: erie.boorman@psy.ox.ac.uk

Summary

The relation between brain structure and function is of fundamental importance in neuroscience. Comparisons between behavioral and brain imaging measures suggest that variation in brain structure correlates with the presence of specific skills[1-3]. Behavioral measures, however, reflect the integrated function of multiple brain regions. Rather than behavior, a *physiological* index of function could be a more sensitive and informative measure with which to compare structural measures. Here, we test for a relationship between a physiological measure of functional connectivity between two brain areas during a simple decision making task and a measure of structural connectivity. Paired-pulse transcranial magnetic stimulation indexed functional connectivity between two regions important for action choices: premotor and motor cortex. Fractional anisotropy (FA), a marker of microstructural integrity, indexed structural connectivity. Individual differences in functional connectivity during action selection show highly specific correlations with FA in localised regions of white matter interconnecting regions including the premotor and motor cortex. Probabilistic tractography[4, 5], a technique for identifying fibre pathways from diffusion-weighted imaging (DWI), reconstructed the anatomical networks linking the component brain regions involved in making decisions. These findings demonstrate a relationship between individual differences in functional and structural connectivity within human brain networks central to action choice.

Results

We employed a novel strategy to test whether a physiological index of functional interactions between brain regions important for action selection correlates with the

microstructural integrity of specific white matter pathways. Because convergent neurophysiological[6, 7], neuroimaging[8-11], and single-pulse TMS[8, 12, 13] evidence has implicated interactions between dorsal premotor cortex (PMd) and primary motor cortex (M1) in the process of externally cued action selection, we focused our investigation on these two regions. We first assessed functional connectivity between PMd and M1 during a particular cognitive state - action selection. We then tested for an association between this measure of functional connectivity and FA values calculated within a white matter network.

Physiological results measured by paired-pulse TMS

One physiological approach to measuring functional connectivity is paired-pulse transcranial magnetic stimulation (TMS). In the paired-pulse TMS protocol we use here, a test pulse over M1 is preceded by a conditioning pulse over contralateral PMd at various inter-pulse intervals (IPIs; Figure 1A). The conditioning pulse modulates the amplitude of motor evoked potentials (MEPs) elicited by the test pulse, depending on the IPI at which the conditioning pulse is delivered[14-16]; this technique has therefore been taken as a measure of functional connectivity between stimulated regions[17].

Recently, paired-pulse TMS has been used to assess functional connectivity between PMd and contralateral M1 during action selection[18, 19]. In a previous experiment, we assessed functional connectivity during an action selection ("choice") task. In this task subjects selected left or right index finger responses on the basis of four learned visuomotor associations (Figure 1B). We recorded MEP amplitudes from the FDI hand muscle contralateral to the stimulated M1 when M1 test pulses were preceded by conditioning pulses over contralateral PMd by an 8ms IPI[14, 16]. In a second condition, we reversed the TMS coils so that both lPMd-rM1 and rPMd-lM1

combinations were tested. The TMS data are reported in full elsewhere[19]. Here, we wished to test how inter-individual variation in a specific TMS measure co-varied with brain structure. The choice of TMS measure was motivated by the results of our previous study. Briefly, MEP amplitudes were significantly facilitated by conditioning pulses at visual stimulus (to TMS) onset asynchronies (SOAs) of 75ms, as reported previously[18](Figure 1C); interaction between SOA and TMS ($F(4,32) = 2.854$, $p=0.039$), corrected post-hoc paired sample t-tests for paired versus single pulse MEPs at 75ms ($t(8)=-2.513$, $p=0.036$). Such facilitatory TMS effects are not directly related in a simple way to the increases in blood oxygenation levels that are measured with functional magnetic resonance imaging. Nevertheless, they likely reflect the co-activation of PMd and M1 during action selection that has been demonstrated to occur in such tasks[10, 11, 13]. Moreover, these effects are specific to action selection; modulation is absent at 75ms in simple movement execution tasks for which subjects do not have to choose between movements and the premotor cortex is significantly less active in such control tasks[8, 10, 11, 13, 19, 20].

To capture this specific facilitatory effect at 75ms during the "choice" task, we first calculated an MEP amplitude ratio between paired and single pulses and then calculated the difference between MEP ratios at SOAs of 75ms and 100ms (see Experimental Procedures). We also repeated these analyses using the MEP ratio between paired and single pulses at 75 ms only. We predicted positive correlations between TMS effects and FA, reflecting increasing FA associated with increasing functional connectivity.

Correlations between TMS measures of functional connectivity and FA

Microstructural properties of human white matter can be interrogated *in vivo* using DWI, which is sensitive to apparent water diffusion properties in brain tissue[21].

DWI takes advantage of the fact that water diffusion is orientation-dependent within tissue characterized by a high degree of directional organization, such as white matter. The orientational dependence of this diffusion can be quantified by *fractional anisotropy* (FA) at each voxel[22-24]. FA has been shown to reflect functionally-relevant microstructural properties of white matter, including axonal architecture, extent of myelination, and density of axonal fibres comprising axonal bundles[21], and has therefore been interpreted as a measure of microstructural integrity[25, 26].

To test whether there was a relationship between functional connectivity and white matter microstructure across subjects, we used tract based spatial statistics (TBSS)[27] to test for local correlations between FA estimates and TMS effect sizes (see Experimental Procedures). Because we were stimulating over PMd and M1 and investigating correlates with action selection signals, this analysis was restricted to a volume of interest (VOI) from a central portion of the brain predicted to mediate these effects.

In both conditions (lPMd-rM1, rPMd-lM1) of our "choice" task, TMS-assessed functional connectivity was positively correlated with FA in white matter tracts connecting premotor-parietal networks. Our multiple regression analysis revealed positive correlations between lPMd-rM1 functional connectivity and FA in clusters underlying lPMd, rPMd, and left sensorimotor cortex, and two clusters in the right SLF ($t>3.35$, $p<0.005$; Figure 2, Table S1). Functional connectivity between rPMd and lM1 was positively correlated with FA in clusters underlying rPMd, bilateral premotor areas extending into supplementary motor areas (SMAs), the CC, the SLF, and the ILF ($t>3.35$, $p<0.005$; Figure 3, Table S1). Using the MEP ratio at 75 ms only as the regressor for the TBSS analyses yielded virtually identical correlations (Figure S1 and S2). Note that within the restricted VOI used for the

TBSS analysis, fewer than 0.5% of white matter skeleton voxels were identified as significant, so these correlations were highly specific. When we repeated these analyses across the whole brain, we found additional correlations restricted to the SLF, extensions of the SLF in the posterior parietal cortex, the genu and splenium of the CC, the uncinate, and an antero-posterior tract bordering the forceps major (Table S1). Notably, disconnection of the temporal and frontal lobes by uncinate transection in non-human primates induces a profound impairment in selecting between motor responses on the basis of a visual cue[28], indicating that this fascicle is functionally related to the "choice" task used here. It is important to note that FA in subregions of the same tract, interconnected tracts or functionally related networks are likely to co-vary, and so these additional correlations may result from inter-regional white matter correlations within the same tract or network, as previously reported for inter-connected grey matter regions [29, 30]. However, using a regressor derived from the PMd-M1 MEP modulation ratio at 100ms (Figure 1C) yielded FA correlations restricted to the corticospinal tracts and not in premotor white matter, the CC, or the SLF. This analysis demonstrates that PMd-M1 MEP modulation at the 75ms time point that is specifically related to the process of action selection is selectively associated with FA in the premotor cortex and its interconnecting fascicles. The correlations reported above all remained significant ($r>0.78$, $p<0.05$) after controlling for age, TMS stimulation intensities for both hemispheres, and skull-cortex distance (see Supplemental Data for further details).

Tractography from white matter regions showing local correlations

To elucidate the white matter tracts in which local regions of FA correlation were found, and the gray matter targets to which they projected, we used these correlated

clusters as seed masks for multi-fibre probabilistic diffusion tractography (PDT)[4, 31].

In the lPMd–rM1 condition, the correlated cluster underlying lPMd generated local premotor and transcallosal paths to white matter underlying contralateral PMd (Figure 2C). Conversely, the cluster underlying rPMd was traced locally within premotor cortex but also inferiorly along the right CST and did not branch into the CC (Figure 2F). The two clusters in the SLF generated paths between posterior parietal and premotor cortex (Figure 2I). Finally, the sensorimotor cluster generated local paths between sensorimotor and premotor cortex. This combined parietal-premotor-contralateral premotor network of connectivity is illustrated in Figure 2J,K.

In the rPMd-lM1 condition, the correlated cluster underlying rPMd also generated local premotor, transcallosal, and right CST paths (Figure 3C). Tractography from the additional clusters underlying premotor areas generated transcallosal tracts targeting homologous regions in the contralateral hemisphere, while the CC cluster generated both transcallosal paths targeting bilateral SMA and left CST paths (Figure 3F). Finally, the SLF cluster was traced between parietal and premotor/prefrontal cortex (Figure 3I). This parietal-premotor-contralateral premotor network of structural connectivity is shown in Figure 3J,K.

Note that our method for visualisation of tracts (Figures 2,3) indicates the maximum number of subjects in whom a tract overlaps at each voxel in standard space and thereby provides a conservative estimate of inter-subject consistency. For example, the maximum overlap of transcallosal tracts from the left PMd cluster shown in Figure 2A indicates that 5 our of 9 subjects overlap at 2, -10, 25, while inspection of individual subject tract maps reveals that transcallosal tracts are generated in 7 out of 9 subjects from the left PMd cluster.

Discussion

We have demonstrated a correlation between natural variation in behavior-specific functional connectivity from PMd to contralateral M1 and microstructural integrity of the specific white matter networks presumed to mediate the physiological effects. The spatial specificity and replicability of the white matter regions showing high correlation in the current study confirms that variation in white matter structure across individuals is associated with variation in function in the same neural system. Such structural-physiological relationships may explain previous reports of correlation between brain structure and behaviour [1-3, 32, 33].

Our "choice" task and similar paradigms have previously been shown to recruit a premotor-parietal network with bilateral activations in PMd and along the intraparietal sulcus (IPS)[8, 10, 11, 13, 20]. We found TMS-assessed functional connectivity during the choice task to correlate with FA specifically in the precentral gyrus white matter, possibly at the white/gray matter boundary, underlying the conditioned PMd, the adjacent SLF connecting IPS and premotor cortex/frontal pars opercularis, and the corpus callosum[34]. We also found correlations in white matter underlying premotor areas that extended to bilateral SMA and sensorimotor cortex, consistent with the finding that BOLD responses during the same choice task extend into these cortical regions[8, 10, 11, 13, 20]. Our physiological probe of FA therefore identified correlations in specific cortico-cortical tracts predicted by previous neuroimaging studies.

It is important to note, however, that within an individual, FA will vary along a tract due to factors such as fibre complexity and compression. Therefore, sensitivity to FA-physiology correlations may vary at different points along a tract. Thus, it is

conceivable that the true extent of pathways involved in this task may be underestimated here.

FA is sensitive to multiple microstructural properties of white matter, including axon density, myelination, and possibly diameter[21, 35]. The functional connectivity-FA correlations we found may be caused by variation in axon density or diameter. Both electromyography (EMG) amplitude and area increase with fibre density in physiological studies of peripheral nerves, and with both fibre density and axon diameter in computer simulations[36, 37]. It is also possible that increased myelination or axon diameter across individuals led to increased or more synchronized axonal conduction velocities, which affected the degree of inter-regional modulation observed.

The electrical conductivity and water self-diffusion tensors are closely related[38, 39], since some of the same geometric tissue properties that lead to increased anisotropic diffusion also lead to increased anisotropic conductivity. It is therefore possible that FA influences passive propagation of the TMS pulse. However, it is widely held that at the intensities used here, TMS excites cortical neurons and interneurons, generating descending volleys trans-synaptically, and not at the level of the axon itself[40]. In addition, the specific latency at which MEP modulation occurred strongly suggests that PMd was functionally interacting with contralateral M1 at this SOA. It is also important to note that we specifically controlled for stimulation thresholds over both hemispheres and skull-cortex distance. Taken together, these points suggest that the correlations we observed were predominately due to a relation between PMd-M1 physiological interactions and FA.

It is imperative to recall that our physiological measures are always of *relative* MEP modulation, rather than absolute MEP amplitudes. Variability in absolute

physiological measures may be confounded with variability in distance between TMS coil and precise brain region even after scalp to brain surface has been considered. The relative modulation measure, for which coil position did not change between the SOAs, may be particularly suitable for comparing against a structural connectivity measure.

With a cross-sectional study, it is not possible to determine the direction of causality between brain structure and function. Innate variation in structural connectivity of the motor system may determine the physiological measure recorded. Alternatively, variation in experience may induce functional plasticity in these motor pathways, which in turn results in measurable structural changes. Animal studies[41] and in-vitro experiments[42] suggest that axonal size or myelination, which are known to modulate FA values[21], may be susceptible to experience-dependent change. Therefore, it is conceivable that variation in experience could result in variation in FA, a conclusion supported by evidence of correlations between FA and hours of musical training experienced by pianists[2]. Future studies could test whether prolonged stimulation of a specific brain pathway, either behaviorally or physiologically, results in both functional and structural plasticity.

The current findings show that regionally specific microstructural features are related to physiological connectivity indices in human subjects during behavior. Such structural-physiological relationships may underlie recently reported individual differences in brain structure and behavior[1-3, 32, 33]. Our approach could be applied to clinical populations, for instance, to help characterize the extent of both the functional and anatomical reorganisation that occurs in response to brain injury or stroke. The present results also suggest that FA could be related to other physiological measures, such as event-related potentials, to further investigate the relationship

between the microstructural integrity of specific anatomical pathways and physiological indices of function.

Experimental Procedures

Subjects

10 healthy, right-handed adults (3 males, ages 23-32) underwent DTI. Two subjects failed to complete one TMS condition (lPMd-rM1 or rPMd-lM1), resulting in 9 subjects per TMS condition. Written informed consent was obtained for all subjects prior to participation in accordance with local ethical approval.

TMS Analysis

The TMS methods are reported in full elsewhere[19] (see Supplemental Experimental Procedures for details).

DWI and TBSS

We acquired diffusion-weighted (2 acquisitions of 60 directions, b-value 1000smm^{-2}, 2.5x2.5x2.5mm^3 voxels, 60 slices) and T1-weighted data using a 1.5T Siemens Sonata MR scanner. Image analysis was carried out and FA values were calculated using FMRIB's diffusion toolbox (FDT) from FMRIB's Software Library (www.fmrib.ox.ac.uk/fsl). To test for correlations between TMS effect sizes and FA values, we employed tract-based spatial statistics (TBSS)[27], which enables statistical comparison of FA values from homologous regions of the FA map across subjects (see Supplemental Experimental Procedures for details).

Correlation with TMS

To test whether there was a relationship between functional connectivity and FA values across subjects, we calculated the difference in MEP ratio between SOAs of 75 and 100ms (i.e., $MEPratio_{75ms}$-$MEPratio_{100ms}$) and used this as a regressor in our

TBSS analysis for both conditions. A GLM approach was used to correlate the TMS effect size for both conditions separately with FA values derived from the group skeleton. We restricted our analyses to the white matter within a central portion of the brain by using a probabilistic tissue type segmentation of the MNI152 template brain, thresholded to include only those voxels classified as white matter in at least 1/3 of the population, and lying between Y= 15 and Y= -25. Having defined this restricted volume of interest and predicted positive correlations, we used a one-tailed statistical threshold $t>3.35$ ($p<0.005$ uncorrected) and a cluster extent threshold of $\geq$10 voxels.

Probabilistic diffusion tractography

Correlated clusters identified using TBSS above were then used as seed masks for Probabilistic Diffusion Tractography (PDT)[4]. PDT estimates a probability distribution function (pdf) on fibre direction at each voxel. A multi-fibre model was fit to the diffusion data at each voxel to allow tracing of fibres through regions of fibre crossing or complexity[31]. These methods are fully described elsewhere[4, 31]. While this model is sufficient to resolve two crossing fibres with the parameters used here, higher field strengths, b-values, and/or more diffusion directions would be necessary to resolve multiple fibre populations of three or more crossing fibres[19, 31]. Here, we drew 25,000 streamline samples from our seeded voxels through these pdfs to form an estimate of the probability distribution of connections from each seeded voxel. When these streamlines reach a voxel in which more than one direction is estimated they follow the direction that is closest to parallel with the direction at which the streamline arrives. Tracts generated by PDT are volumes wherein values at each voxel represent the number of samples (or streamlines) that passed through that voxel. To eliminate spurious connections, tractography in individual subjects was thresholded to include only voxels through which at least 50 samples had passed (out

of 25,000). These individual tracts were then binarised and summed across subjects to produce group probability maps for each pathway, where each voxel value represents the number of subjects in whom the pathway passes through that voxel. For visualisation, these group probability maps were then thresholded to display only those paths that were present in a minimum of ~40% and a maximum of 100% of subjects. These thresholded group probability maps from significant clusters were then summed to construct a composite connectivity network.

Acknowledgements

We are grateful for financial support from the Wellcome Trust (EDB, HJB), MRC and Royal Society (MFSR), and Stevenson Junior Research Fellowship, University College Oxford (JOS). We wish to thank TEJ Behrens for producing the tractography algorithm and helpful comments and SM Smith and S Jbabdi for help with TBSS analysis.

References

1. Maguire, E.A., Gadian, D.G., Johnsrude, I.S., Good, C.D., Ashburner, J., Frackowiak, R.S., and Frith, C.D. (2000). Navigation-related structural change in the hippocampi of taxi drivers. Proc Natl Acad Sci U S A *97*, 4398-4403.
2. Bengtsson, S.L., Nagy, Z., Skare, S., Forsman, L., Forssberg, H., and Ullen, F. (2005). Extensive piano practicing has regionally specific effects on white matter development. Nat Neurosci *8*, 1148-1150.
3. Gaser, C., and Schlaug, G. (2003). Brain structures differ between musicians and non-musicians. J Neurosci *23*, 9240-9245.
4. Behrens, T.E., Woolrich, M.W., Jenkinson, M., Johansen-Berg, H., Nunes, R.G., Clare, S., Matthews, P.M., Brady, J.M., and Smith, S.M. (2003). Characterization and propagation of uncertainty in diffusion-weighted MR imaging. Magn Reson Med *50*, 1077-1088.
5. Behrens, T.E., Johansen-Berg, H., Woolrich, M.W., Smith, S.M., Wheeler-Kingshott, C.A., Boulby, P.A., Barker, G.J., Sillery, E.L., Sheehan, K., Ciccarelli, O., Thompson, A.J., Brady, J.M., and Matthews, P.M. (2003). Non-invasive mapping of connections between human thalamus and cortex using diffusion imaging. Nat Neurosci *6*, 750-757.

6. Cisek, P., and Kalaska, J.F. (2005). Neural correlates of reaching decisions in dorsal premotor cortex: specification of multiple direction choices and final selection of action. Neuron *45*, 801-814.
7. Wise, S.P., Boussaoud, D., Johnson, P.B., and Caminiti, R. (1997). Premotor and parietal cortex: corticocortical connectivity and combinatorial computations. Annu Rev Neurosci *20*, 25-42.
8. Johansen-Berg, H., Rushworth, M.F., Bogdanovic, M.D., Kischka, U., Wimalaratna, S., and Matthews, P.M. (2002). The role of ipsilateral premotor cortex in hand movement after stroke. Proc Natl Acad Sci U S A *99*, 14518-14523.
9. Schluter, N.D., Rushworth, M.F., Mills, K.R., and Passingham, R.E. (1999). Signal-, set-, and movement-related activity in the human premotor cortex. Neuropsychologia *37*, 233-243.
10. Amiez, C., Kostopoulos, P., Champod, A.S., and Petrides, M. (2006). Local morphology predicts functional organization of the dorsal premotor region in the human brain. J Neurosci *26*, 2724-2731.
11. Grol, M.J., de Lange, F.P., Verstraten, F.A., Passingham, R.E., and Toni, I. (2006). Cerebral changes during performance of overlearned arbitrary visuomotor associations. J Neurosci *26*, 117-125.
12. Schluter, N.D., Rushworth, M.F., Passingham, R.E., and Mills, K.R. (1998). Temporary interference in human lateral premotor cortex suggests dominance for the selection of movements. A study using transcranial magnetic stimulation. Brain *121 (Pt 5)*, 785-799.
13. Rushworth, M.F., Johansen-Berg, H., Gobel, S.M., and Devlin, J.T. (2003). The left parietal and premotor cortices: motor attention and selection. Neuroimage *20 Suppl 1*, S89-100.
14. Mochizuki, H., Huang, Y.Z., and Rothwell, J.C. (2004). Interhemispheric interaction between human dorsal premotor and contralateral primary motor cortex. J Physiol *561*, 331-338.
15. Baumer, T., Bock, F., Koch, G., Lange, R., Rothwell, J.C., Siebner, H.R., and Munchau, A. (2006). Magnetic stimulation of human premotor or motor cortex produces interhemispheric facilitation through distinct pathways. J Physiol *572*, 857-868.
16. Koch, G., Franca, M., Mochizuki, H., Marconi, B., Caltagirone, C., and Rothwell, J.C. (2007). Interactions between pairs of transcranial magnetic stimuli over the human left dorsal premotor cortex differ from those seen in primary motor cortex. J Physiol *578*, 551-562.
17. Baumer, T., Rothwell, J.C., and Munchau, A. (2003). Functional connectivity of the human premotor and motor cortex explored with TMS. Suppl Clin Neurophysiol *56*, 160-169.
18. Koch, G., Franca, M., Del Olmo, M.F., Cheeran, B., Milton, R., Alvarez Sauco, M., and Rothwell, J.C. (2006). Time course of functional connectivity between dorsal premotor and contralateral motor cortex during movement selection. J Neurosci *26*, 7452-7459.
19. O'Shea, J., Sebastian, C., Boorman, E.D., Johansen-Berg, H., Rushworth, M.F.S. (in press). Functional specificity of dorsal premotor/motor cortical interactions during action selection. Eur J Neurosci.
20. O'Shea, J., Johansen-Berg, H., Trief, D., Gobel, S., and Rushworth, M.F. (2007). Functionally specific reorganization in human premotor cortex. Neuron *54*, 479-490.

21. Beaulieu, C. (2002). The basis of anisotropic water diffusion in the nervous system - a technical review. NMR Biomed *15*, 435-455.
22. Basser, P.J., Mattiello, J., and LeBihan, D. (1994). Estimation of the effective self-diffusion tensor from the NMR spin echo. J Magn Reson B *103*, 247-254.
23. Basser, P.J., and Pierpaoli, C. (1996). Microstructural and physiological features of tissues elucidated by quantitative-diffusion-tensor MRI. J Magn Reson B *111*, 209-219.
24. Johansen-Berg, H., and Behrens, T.E. (2006). Just pretty pictures? What diffusion tractography can add in clinical neuroscience. Curr Opin Neurol *19*, 379-385.
25. Klingberg, T., Hedehus, M., Temple, E., Salz, T., Gabrieli, J.D., Moseley, M.E., and Poldrack, R.A. (2000). Microstructure of temporo-parietal white matter as a basis for reading ability: evidence from diffusion tensor magnetic resonance imaging. Neuron *25*, 493-500.
26. Head, D., Buckner, R.L., Shimony, J.S., Williams, L.E., Akbudak, E., Conturo, T.E., McAvoy, M., Morris, J.C., and Snyder, A.Z. (2004). Differential vulnerability of anterior white matter in nondemented aging with minimal acceleration in dementia of the Alzheimer type: evidence from diffusion tensor imaging. Cereb Cortex *14*, 410-423.
27. Smith, S.M., Jenkinson, M., Johansen-Berg, H., Rueckert, D., Nichols, T.E., Mackay, C.E., Watkins, K.E., Ciccarelli, O., Cader, M.Z., Matthews, P.M., and Behrens, T.E. (2006). Tract-based spatial statistics: voxelwise analysis of multi-subject diffusion data. Neuroimage *31*, 1487-1505.
28. Eacott, M.J., and Gaffan, D. (1992). Inferotemporal-frontal Disconnection: The Uncinate Fascicle and Visual Associative Learning in Monkeys. Eur J Neurosci *4*, 1320-1332.
29. Mechelli, A., Friston, K.J., Frackowiak, R.S., and Price, C.J. (2005). Structural covariance in the human cortex. J Neurosci *25*, 8303-8310.
30. Lerch, J.P., Worsley, K., Shaw, W.P., Greenstein, D.K., Lenroot, R.K., Giedd, J., and Evans, A.C. (2006). Mapping anatomical correlations across cerebral cortex (MACACC) using cortical thickness from MRI. Neuroimage *31*, 993-1003.
31. Behrens, T.E., Berg, H.J., Jbabdi, S., Rushworth, M.F., and Woolrich, M.W. (2007). Probabilistic diffusion tractography with multiple fibre orientations: What can we gain? Neuroimage *34*, 144-155.
32. Toosy, A.T., Ciccarelli, O., Parker, G.J., Wheeler-Kingshott, C.A., Miller, D.H., and Thompson, A.J. (2004). Characterizing function-structure relationships in the human visual system with functional MRI and diffusion tensor imaging. Neuroimage *21*, 1452-1463.
33. Tuch, D.S., Salat, D.H., Wisco, J.J., Zaleta, A.K., Hevelone, N.D., and Rosas, H.D. (2005). Choice reaction time performance correlates with diffusion anisotropy in white matter pathways supporting visuospatial attention. Proc Natl Acad Sci U S A *102*, 12212-12217.
34. Rushworth, M.F., Behrens, T.E., and Johansen-Berg, H. (2006). Connection patterns distinguish 3 regions of human parietal cortex. Cereb Cortex *16*, 1418-1430.
35. Takahashi, M., Hackney, D.B., Zhang, G., Wehrli, S.L., Wright, A.C., O'Brien, W.T., Uematsu, H., Wehrli, F.W., and Selzer, M.E. (2002). Magnetic resonance microimaging of intraaxonal water diffusion in live excised lamprey spinal cord. Proc Natl Acad Sci U S A *99*, 16192-16196.

36. Finsterer, J., and Fuglsang-Frederiksen, A. (2000). Concentric needle EMG versus macro EMG I. Relation in healthy subjects. Clin Neurophysiol *111*, 1211-1215.
37. Nandedkar, S., and Stalberg, E. (1983). Simulation of macro EMG motor unit potentials. Electroencephalogr Clin Neurophysiol *56*, 52-62.
38. Tuch, D.S., Wedeen, V.J., Dale, A.M., George, J.S., and Belliveau, J.W. (2001). Conductivity tensor mapping of the human brain using diffusion tensor MRI. Proc Natl Acad Sci U S A *98*, 11697-11701.
39. Haueisen, J., Tuch, D.S., Ramon, C., Schimpf, P.H., Wedeen, V.J., George, J.S., and Belliveau, J.W. (2002). The influence of brain tissue anisotropy on human EEG and MEG. Neuroimage *15*, 159-166.
40. Mills, K.R. (1999). Magnetic Stimulation of the Human Nervous System (New York: Oxford University Press).
41. Juraska, J.M., and Kopcik, J.R. (1988). Sex and environmental influences on the size and ultrastructure of the rat corpus callosum. Brain Res *450*, 1-8.
42. Demerens, C., Stankoff, B., Logak, M., Anglade, P., Allinquant, B., Couraud, F., Zalc, B., and Lubetzki, C. (1996). Induction of myelination in the central nervous system by electrical activity. Proc Natl Acad Sci U S A *93*, 9887-9892.

Figure Legends

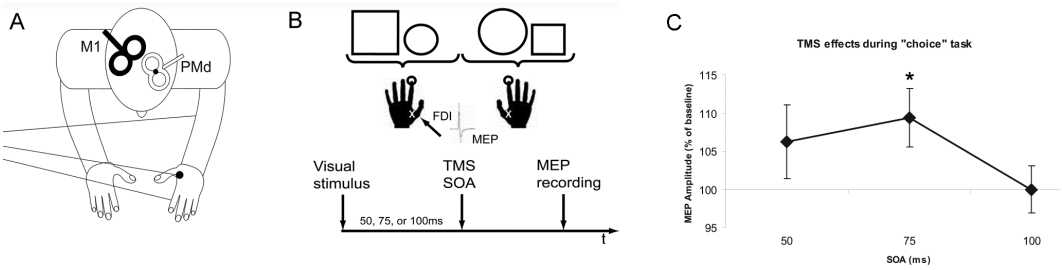

Figure 1. TMS experimental setup and results. (A) Conditioning pulses were applied over PMd and test pulses, over contralateral M1. In this example, coils are positioned over lPMd and rM1. We tested both lPMd-rM1 and rPMd-lM1. MEPs were recorded from active electrodes over FDI hand muscle (indicated by the black circle) contralateral to the stimulated M1. (B) During the "choice" task, one of four shape stimuli was presented on each trial, and remained on the screen until subjects made a button-press response with the index finger of the right or left hand (circled) according to a learned rule. TMS was delivered at SOAs of 50, 75, or 100ms after the

onset of the visual stimulus. On single-pulse TMS trials, a single TMS pulse was applied to M1; on paired-pulse TMS trials a conditioning TMS pulse was applied over contralateral PMd 8ms prior to the M1 pulse, while motor-evoked potentials (MEPs) were recorded. Redrawn from[19]. (C) Effects during behavioral choice: Normalised mean amplitude MEPs recorded from FDI muscle contralateral to stimulated M1. Error bars represent ±SEM. Redrawn from[19].

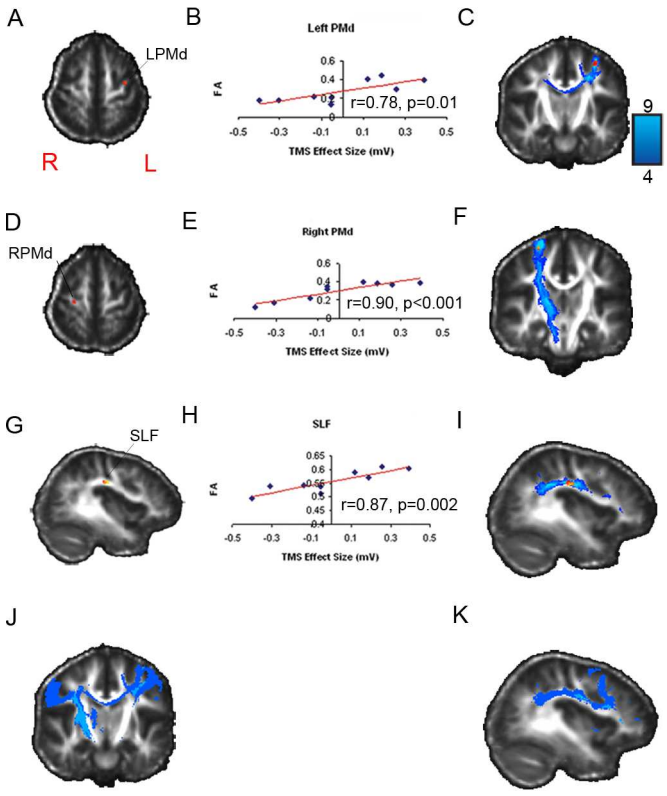

Figure 2. Local correlations between FA and functional connectivity between lPMd and rM1 during the "choice" task, and probabilistic tractography from local areas of correlation. (A,D,G): Clusters showing significant positive correlations between TMS effect sizes and FA when conditioning pulses were applied over lPMd and test pulses over rM1, overlaid on the mean FA image from all participants. T-statistic images are thresholded at t>3.35 and cluster extent ≥10 voxels. Suprathreshold clusters are then

dilated by one voxel for improved visualisation. Color scale represents t-score from low (t=3.35, red) to high (yellow). Images are displayed according to radiological convention. (B,E,H): Scatterplots showing individual FA and TMS values for selected clusters. (C,F,I,J,K): Group probability maps of tracts generated by PDT from positively correlated clusters when stimulating over lPMd-rM1. Maps were overlaid onto the mean FA image from all participants and paths are color-coded according to whether the number of subjects containing that path is high (light blue) or low (dark blue) according to the color scale. Axial section illustrating correlation in white matter underlying lPMd (labeled LPMd) (A), scatterplot of individual FA values from lPMd cluster shown in (A) and TMS values (B), and local premotor and transcallosal tracts generated from lPMd cluster (C). Axial section of correlations in white matter underlying rPMd (labeled RPMd) (D), scatterplot of FA and TMS values from the rPMd cluster (E), and local premotor and CST tracts traced by PDT from the rPMd cluster (F). Sagittal section of SLF correlated cluster (G), scatterplot of FA and TMS values from the SLF cluster (H), and SLF tract projecting from posterior parietal cortex to PMd generated from the SLF cluster (I). (J,K) Group probability map displaying the combined network of thresholded and summed tracts generated by PDT from all voxels within positively correlated clusters when stimulating over lPMd-rM1, shown in coronal section and sagittal sections.

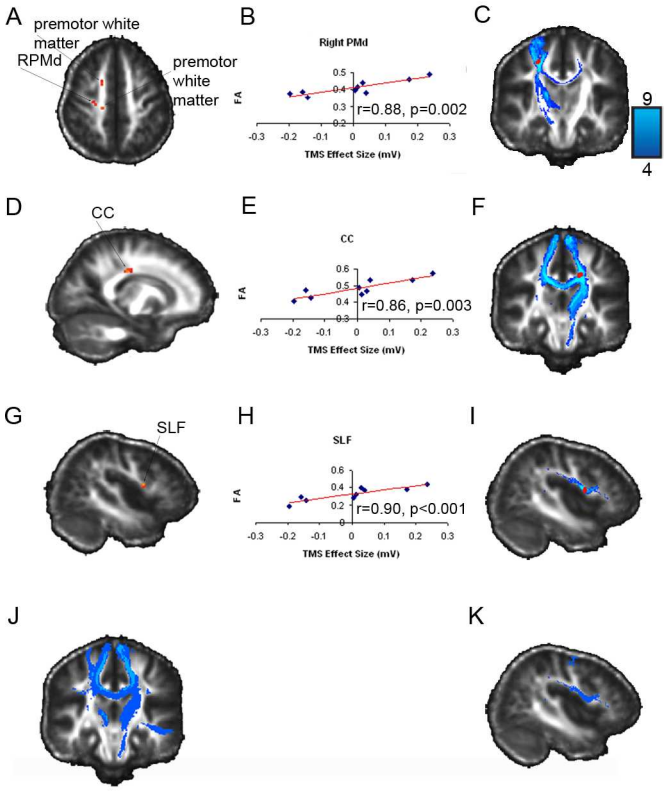

Figure 3. Local correlations between FA and functional connectivity between rPMd and lM1 during action selection and probabilistic tractography from local areas of correlation. Images were produced and displayed using the same methods as in Figure 2. Axial section illustrating correlations in premotor white matter including white matter underlying rPMd (labeled RPMd) and other premotor regions (A), scatterplot between FA and TMS values (B), and tractography showing local premotor, transcallosal, and corticospinal paths (C). Sagittal section of CC cluster (D), scatterplot of FA and TMS values (E), and callosal paths targeting SMA and a left CST path (F) generated by PDT. Sagittal section of SLF correlation (G), scatterplot between FA and TMS values (H), and SLF tract coursing between the posterior parietal and prefrontal cortex (I). (J,K) Coronal and sagittal sections of the group probability map, generated by thresholding and summing all tracts generated by PDT, illustrating a combined network of connectivity.